Chemical Physics Letters 486 (2010) 32–36

Contents lists available at ScienceDirect

Chemical Physics Letters

journal homepage: www.elsevier.com/locate/cplett

Specific interactions in partially miscible polycarbonate (PC)/poly (methyl methacrylate) (PMMA) blends

A.K. Singh [a,b], R.K. Mishra [a], Rajiv Prakash [a], Pralay Maiti [a], Akhilesh Kumar Singh [a], Dhananjai Pandey [a,*]

[a] School of Materials Science and Technology, Institute of Technology, Banaras Hindu University, Varanasi 221 005, India
[b] Moserbaer India Limited, 66 Udyog Vihar, Greater Noida, India

ARTICLE INFO

Article history:
Received 26 September 2009
In final form 28 December 2009
Available online 4 January 2010

ABSTRACT

Blends of bisphenol A polycarbonate and poly(methyl methacrylate) have been prepared by solution casting technique using tetrahydrofuran as a solvent. These blends are characterized using DSC, TGA, FT-IR and powder X-ray diffraction techniques. The differential scanning calorimetric and XRD results reveal large crystallinity in the solution cast PC and PC/PMMA blends which decreases with increasing PMMA content. Coherently scattering domain size, on the other hand, increases with increasing PMMA content. Our XRD results reveal that the strongest peak of PC shifts to lower 2θ angles in the PC/PMMA blends indicating the presence of specific interactions between the PC and PMMA phases.

1. Introduction

In recent years, there has been enormous interest in multiphase polymer blends due to the possibility of simultaneously exploiting the attractive features of each blend component [1,2]. Polymer blends have a broad range of technological and scientific applications. Blends of bisphenol A polycarbonates (PC) with poly(methyl methacrylate) (PMMA) have received considerable attention [3–11] because of their potential application as gas separation membrane, pearl material, substrate of the optical data storage discs, packaging material, etc. [12].

PC/PMMA blends are generally prepared by melt extrusion [13–18] or solution casting [3–12,19–32] techniques with or without compatibilizers. The issue of PC/PMMA blend miscibility has been extensively investigated by many polymer research groups. However, it still lacks unanimity [3–12,19–32]. Kim and Burns [9] determined the interaction parameters for PC/PMMA blends and proposed that it is a partially miscible system. However, several workers have claimed miscibility in the PC/PMMA blend on the basis of observation of single glass transition temperature (T_g), especially in solution cast blends.

Saldanha and Kyu [6] studied the effect of various solvents on PC/PMMA blend miscibility and showed that tetrahydrofuran (THF) processed blends at non-ambient temperature exhibit single T_g which varies systematically with composition. Woo and Su [29], Butzbach and Wendorff [4], Kyu and Saldanha [23–25] and Agari et al. [3] also observed single glass transition temperature (T_g) in the first DSC run of THF solution cast PC/PMMA blends which varies systematically with PMMA content. Two clear and distinguishable T_gs have been reported in the second run for the intermediate compositions containing 40–60% and 30–70% PC by Woo and Su [29] and Saldanha and Kyu [6], respectively. They have shown that PC/PMMA blends are stable up to ~240 °C above which phase separation takes place. On the other hand, Chiou et al. [5] have reported that PC/PMMA blends exhibit single broad glass transition for low PMMA content (up to ~30% PMMA content), which does not shift with the PMMA content appreciably. However, their thermograms for the second run show melting peak along with T_g for the blend compositions, but not for pure PC and PMMA, suggesting PMMA induced crystallization of the blend. Woo and Su [10,29] and Nishimoto et al. [28] have proposed that non-observation of the second T_g in the first run of these blends is due to the presence of microheterogeneities on a 100–300 Å scale and does not in any way indicate thermodynamic miscibility. This non-equilibrium microheterogeneous state results from rapid removal of solvents leading to kinetic entrapment of the minority phase in the entangled chain conformation of the majority phase.

The controversies about miscibility in the solution cast PC/PMMA blends has originated from the sensitivity limits of the differential scanning calorimetry and difference in blend preparation conditions. Extensive literature review has revealed that the investigations on PC/PMMA blends have been mainly carried out using DSC, light scattering and SEM techniques. There is no report of a comprehensive X-ray diffraction study of these blends. Keeping this in mind, we have undertaken a combined XRD, DSC, TGA, and FT-IR study of PC/PMMA blends prepared using THF as a solvent in the whole composition range form PC to PMMA end at a non-ambient temperature. Our XRD results reveal that the strongest peak of PC shifts to lower angles in the PC/PMMA blends indicating the presence of specific interactions between the PC and PMMA phases. The coherently scattering crystallite (domain) size

* Corresponding author.
E-mail address: dpandey_bhu@yahoo.co.in (D. Pandey).

0009-2614/$ - see front matter © 2009 Elsevier B.V. All rights reserved.
doi:10.1016/j.cplett.2009.12.072

determined from the most prominent crystalline peak of PC and PC/PMMA blends (for PC rich end) increases with increasing PMMA content further suggesting interactions between the PC and PMMA phases in the blends. Both XRD and DSC data reveal large crystallinity of solution cast PC which decreases with increasing PMMA content in the PC/PMMA blend compositions.

2. Experimental

PMMA (Mol. Weight 15,000, Himedia), PC (Makrolon 2215 Mol. weight 22,000, Bayer), and tetrahydrofuran (Spectrochem) were used for solution blending.

PC/PMMA blends in different weight ratios were prepared by solution casting method. Tetrahydrofuran was used as solvents for all the blend compositions. Blends containing polymer fractions 100/0, 90/10, 80/20, 70/30, 60/40, 50/50, 40/60, 30/70, 20/80, 10/90 and 0/100 in wt.% of PC/PMMA, henceforth denoted as PC, PC/10PMMA, PC/20PMMA, PC/30PMMA, PC/40PMMA, PC/50PMMA, PC/60PMMA PC/70PMMA, PC/80PMMA, PC/90PMMA and PMMA, respectively, were prepared in this work. Blends were prepared by dissolving the predetermined quantity of polymers in THF at 50 °C and homogenized for 4 h in closed environment followed by sonication for 10 min. After that, the solutions were cast in covered petri dishes for controlled evaporation for overnight. Finally, blend films were dried in vacuum oven at 70 °C for removal of the remaining solvents.

Powder XRD patterns were recorded using an 18 kW Cu rotating anode based high resolution Rigaku powder diffractometer fitted with a curved crystal monochromator in the diffracted beam. Data were obtained from $2\theta = 5°$ to 60° at a scanning speed of 3°/min.

Thermal analyses were carried out using a DSC (Mettler-Toledo 832) at a heating rate of 20 °C/min under nitrogen atmosphere. The DSC was calibrated with indium before use.

Thermogravimetric analyses were done with Perkin Elmer TGA at a heating rate of 20 °C/min to measure the degradation temperature.

FT-IR spectroscopic analyses of the samples were conducted using Perkin Elmer FT-IR spectrometer (model: Spectrum RSi) from 400 to 4000 cm^{-1} with a resolution of 4 cm^{-1}.

3. Result and discussion

DSC thermograms of as-cast PC, PMMA and their blends with different PMMA content are shown in Fig. 1. PC shows an endothermic peak at ~240 °C corresponding to its melting point whereas PMMA exhibits no such peak due to the glassy nature of PMMA. As the PMMA content increases melting peak shows broadening suggesting the variation of heat of fusion with the PMMA content. In PC/80PMMA and PC/90PMMA there is no clear signature of melting peak due to the higher PMMA content. In contrast to the observation of Saldanha and Kyu [6] and Hsu [30] who reported both T_g and melting peaks, we observe only melting peak in the first DSC run. This may be probably due to the larger thickness of PC/PMMA blend films in our case which promotes the crystallinity and suppresses the T_g. T_g is more commonly observed in thinner films [10]. The heat of fusion obtained from the melting peak area in the DSC thermograms for the PC/PMMA blends is shown as an inset of Fig. 1. It is evident from the inset that the crystallinity of PC/PMMA decreases with increasing PMMA content. This is very much on expected lines in view of the glassy nature of PMMA.

In order to check the miscibility of the blends we carried out the second DSC run of the as cast samples. Before the second DSC runs, the samples were heated up to 300 °C and then quenched to room temperature. Fig. 2 shows the second DSC run thermograms of PC, PMMA and their blends. PC/10PMMA and PC/20PMMA show single glass transition with a T_g slightly less than the glass transition temperature of pure PC. PC/70PMMA, PC/80PMMA and PC/90PMMA also show single T_g which is slightly higher than the T_g of PMMA.

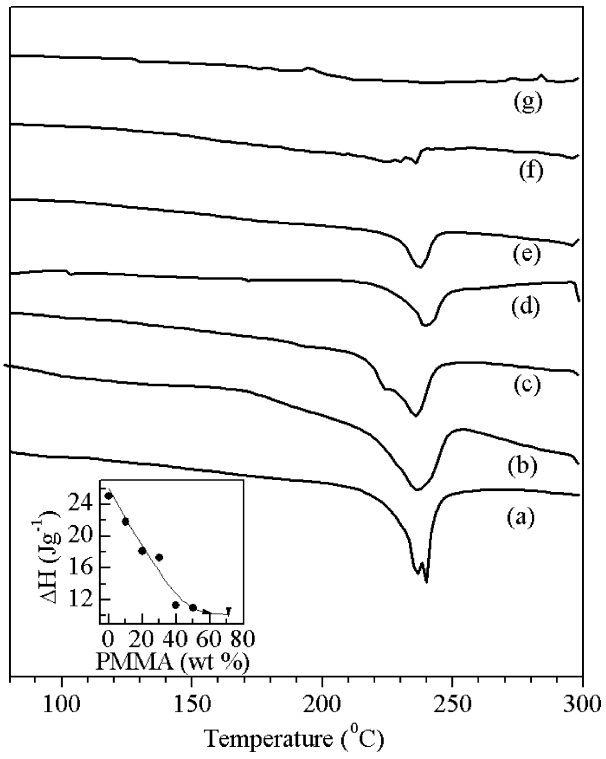

Fig. 1. DSC thermograms (first run) of as-cast PC/PMMA blends prepared using THF: (a) pure PC, (b) PC/10PMMA, (c) PC/30PMMA, (d) PC/40PMMA, (e) PC/60PMMA, (f) PC/80PMMA, and (g) pure PMMA. Inset: PC heat of fusion, as measured by the endothermic melting peak in DSC thermograms.

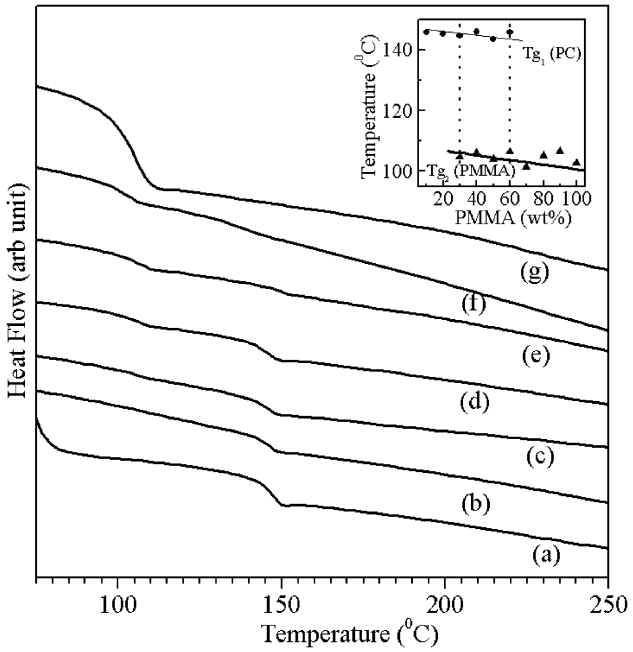

Fig. 2. DSC thermograms (second run) of quenched PC/PMMA blends prepared using THF solvent: (a) pure PC, (b) PC/10PMMA, (c) PC/20PMMA, (d) PC/30PMMA, (e) PC/60PMMA, (f) PC/70PMMA, and (g) pure PMMA. Inset: Variation of T_g (PC) and T_g (PMMA) with PMMA content in PC/PMMA blends.

The blends having PMMA content between 30 and 60 wt.%, on the other hand, show two distinct T_gs which is in broad agreement with the findings of Woo and Su [29] and Saldanha and Kyu [6]. The lower T_g can be easily attributed to the PMMA-rich phase while the higher T_g due to the PC-rich phase. Simple calculation of ΔH_{GT} for the blends using the linear mixture rule shows that ΔH_{GT} for the minority phase in the blends is three orders of magnitude higher than the resolution of the DSC. Had the minority phase been segregated, its glass transition should have been discernible in the DSC scan. The fact that it is not so suggests that the minority phase is homogeneously dispersed in the matrix of the majority phase. The absence of the segregation may be due to the kinetic entrapment of the minority phase and/or due to possible interaction between the PC and PMMA phases. The variation of the glass transition temperature of PC/PMMA blends with PMMA content is shown in the inset of Fig. 2. A linear curve fitting to the observed data points for T_g reveals that as the PMMA content increases, both T_g (PC) and T_g (PMMA) decrease, although only by a very small amount. This small decrease in T_g may be due to week interaction developing between the phenyl rings of PC and carbonyl group of the PMMA phase [4].

TGA curves of PC/PMMA blends for different PMMA content are shown in Fig. 3. The degradation temperature of pure PC, PC/10PMMA, PC/30PMMA, PC/50PMMA and pure PMMA corresponding to 5% degradation are found to be 423, 381, 349, 322 and 199 °C, respectively. The degradation temperature has been plotted in the inset of Fig. 3 as a function of PMMA content. It shows that as the PMMA content increases the degradation temperature decreases linearly. This further indicates specific interactions between PC and PMMA phases.

Fig. 4 shows the FT-IR spectra of PC/PMMA blends along with those for pure PC and PMMA in the wave-number range 1000–2500 cm^{-1}. The stretching vibration peak of carbonyl group occurs at 1773 cm^{-1} and 1733 cm^{-1} in pure PC and PMMA, respectively [19]. For all the blend compositions, the stretching vibration peak of carbonyl groups is a doublet corresponding to the PC and PMMA carbonyl group. The shift in the peak position of the carbonyl group of the PC is rather negligible. However the carbonyl group of PMMA is shifted in the blends by about 6–10 cm^{-1}. This shift, although small, may be due to the week interactions developing between PC and PMMA. The relative intensity of the two carbonyl group peaks varies systematically with composition, as expected.

We now turn to the results of XRD studies. The XRD patterns of the as cast films of PC, PMMA and their blends are shown in Fig. 5. The XRD pattern of pure PC shows three prominent peaks posi-

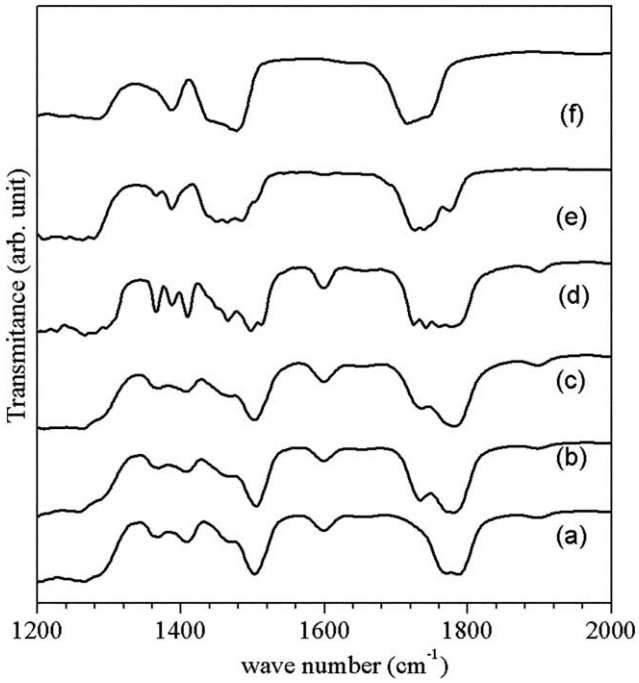

Fig. 4. FT-IR spectra of (a) pure PC, (b) PC/10PMMA, (c) PC/20PMMA, (d) PC/60PMMA, (e) PC/80PMMA, and (f) pure PMMA.

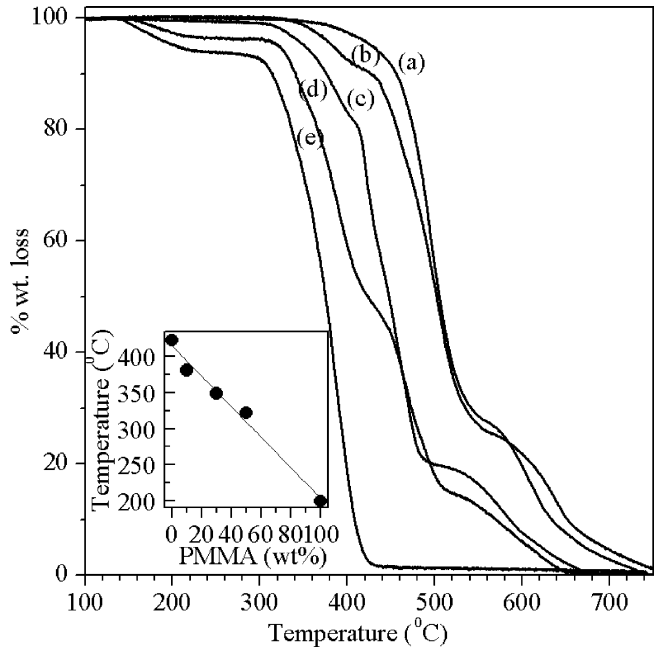

Fig. 3. TGA curve of PC/PMMA blends: (a) pure PC, (b) PC/10PMMA,(c) PC/30PMMA, (d) PC/50PMMA blend, and (e) pure PMMA. Inset shows the temperature of 5% degradation as a function of PMMA content.

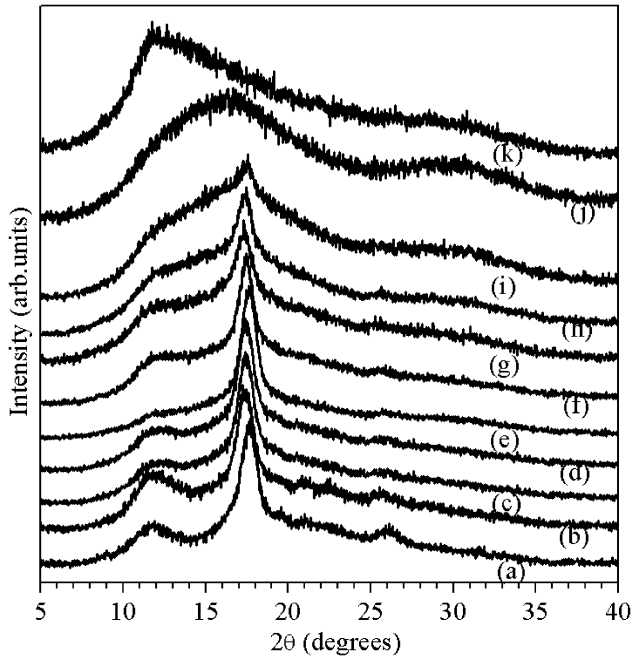

Fig. 5. Powder XRD pattern of as-cast PC/PMMA blend films: (a) pure PC, (b) PC/10PMMA, (c) PC/20PMMA, (d) PC/30PMMA, (e) PC/40PMMA, (f) PC/50PMMA, (g) PC/60PMMA, (h) PC/70PMMA, (i) PC/80PMMA, (j) PC/90PMMA, and (k) pure PMMA.

tioned at $2\theta \approx 12°$, 17.7° and 26° which may be attributed to the interference along the axis of the main chain segment, interference between chains and short range correlations between phenyl groups on neighbouring chains, respectively [33,34]. The improved resolution of the peak positioned at $2\theta \approx 12°$ and 26° is due to the pronounced texturing of the films. As PMMA content increases, the sharp peak at $2\theta \sim 17.2°$ characteristic of PC shows increasingly more asymmetric broadening on the lower 2θ side whereas the other prominent peak positioned at $2\theta \sim 12°$ gets smeared out and overlaps with the characteristic peak of PMMA positioned at $2\theta \sim 12.7°$. As a result, the overall peak position of this smeared peak shifts gradually away from PC position towards the PMMA position indicating interaction between the two phases. Based on a theoretical modelling of the molecular interactions between PC and PMMA, it has been suggested [4] that these interactions comprise Coulombic part and a van der Waals part with latter dominating over the former. This interaction develops between the phenyl rings and the carbonyl group in PC/PMMA blend.

In order to study the solvent induced crystallinity developed in the as cast blends, we crushed the films to fine powders to get rid of the texturing. The powder XRD profiles obtained from such powders is shown in Fig. 6. We have taken the powder XRD data for blends up to 30% PMMA content because the films for higher PMMA content were more ductile and it was not possible to convert them in powder form. From Fig. 6 it is evident that as the PMMA content increases, the sharp peak at $2\theta \sim 17.2°$ characteristic of PC shows increasingly more asymmetric broadening on the lower 2θ side. This broadening is due to the overlap of the broad PMMA peak, which in pure system occurs around $2\theta \sim 12.7°$. The inset of Fig. 6 shows that the position of the strongest peak of PC, at $2\theta \sim 17.22°$, is considerably shifted towards lower two-theta values with increasing PMMA content in the blend compositions. This shift shows linear dependence on composition. Thus in agreement with DSC, TGA and FT-IR findings, powder XRD data also supports the presence of interactions between PC and PMMA phases as revealed by shifting peak positions shown in the inset.

The crystallinity of the blends is most likely a kinetic effect induced by the slow rate of evaporation of the solvent. We have determined the crystallinity of the blends by de-convoluting the powder XRD profiles shown in Fig. 6. For this, we have used Lorentzian peak shape for all the peaks of PC, as use of Gaussian peak shape gave rather poor fit. The number of PC peaks used by us for deconvolution matches with the number of peaks given in Ref. [35]. We have fixed the positions of all the peaks except the strongest peak of PC at $2\theta \sim 17.22°$ and refined the peak area and full width and half maxima (FWHM) in the least squares sense to obtain best fit between the calculated and observed profiles. The observed, fitted and difference profiles are shown in Fig. 7. The nearly flat difference profiles confirm excellent fits. The crystallinity of PC and PC/PMMA blends was determined using volume fraction method [36]. The variation of the crystallinity with PMMA content is shown in the inset (a) of Fig. 7. It is evident from this figure that as a result of solution casting pure PC shows surprisingly very high degree of crystallinity (~35%). ~9% and ~20% crystallinity of PC has been reported by Ouyang and Wu [35] and Font and Muntasell [37] for acetone vapour evaporated and ball milled PC, respectively. Recently Yoo et al. [38] have reported ~35% crystallinity by sonocrystallization of polymer melts. Our crystallinity value for pure PC is close to that obtained by Yoo et al. It is observed that as the PMMA content increases, the crystallinity of PC/PMMA blend decreases linearly which is attributed to the glassy nature of PMMA. This is also supported by heat of fusion data obtained by DSC (see inset of Fig. 1). Fig. 8 shows the variation of heat of fusion obtained by DSC with crystallinity determined by XRD of the PC/PMMA blends. This figure reveals a linear relationship between the heat of fusion and crystallinity of PC/PMMA blends confirming the consistency of both the findings.

We also obtained the coherently scattering crystallite (domain) size of PC and PC/PMMA blends using Scherer equation for the characteristic peak of PC at $2\theta \sim 17.22°$. This equation in its most general form can be written as [39]:

$$\langle D \rangle = 1.33\lambda/(\cos\theta \cdot \beta(2\theta)), \quad (1)$$

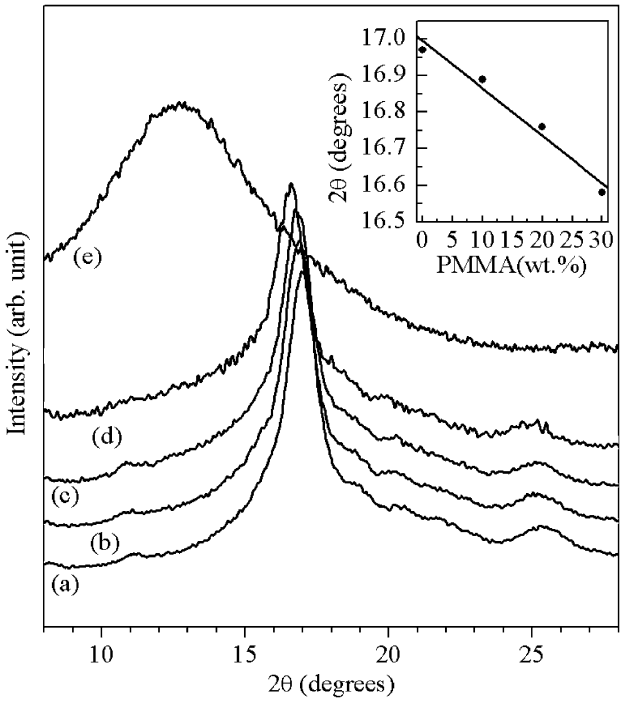

Fig. 6. Powder XRD pattern of as-cast PC/PMMA blend recorded on powder: (a) pure PC, (b) PC/10PMMA, (c) PC/20PMMA, (d) PC/30PMMA, and (e) pure PMMA. Inset shows the peak position of the most prominent PC peak as a function of PMMA content.

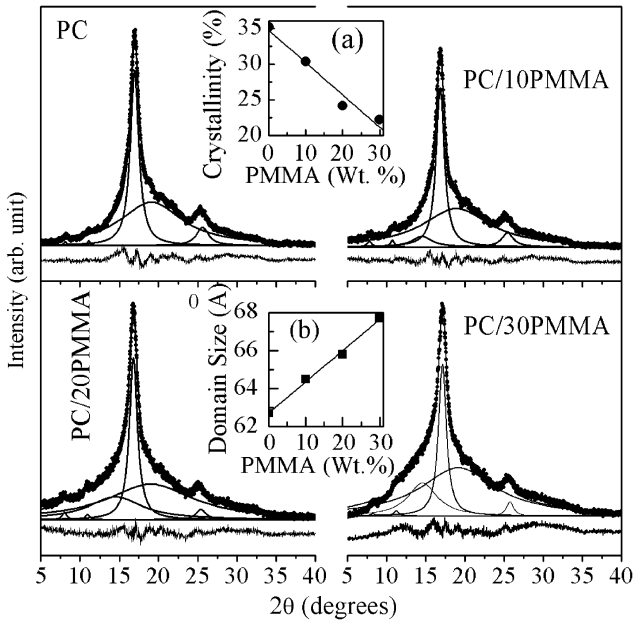

Fig. 7. Multipeak Lorenzian fits for XRD profiles of PC/PMMA blends. Lower pattern below the deconvoluted peaks shows the difference between the observed and calculated patterns. Inset: Variation of PC/PMMA blend crystallinity (a) and coherently scattering domain size of PC (b) with PMMA content.

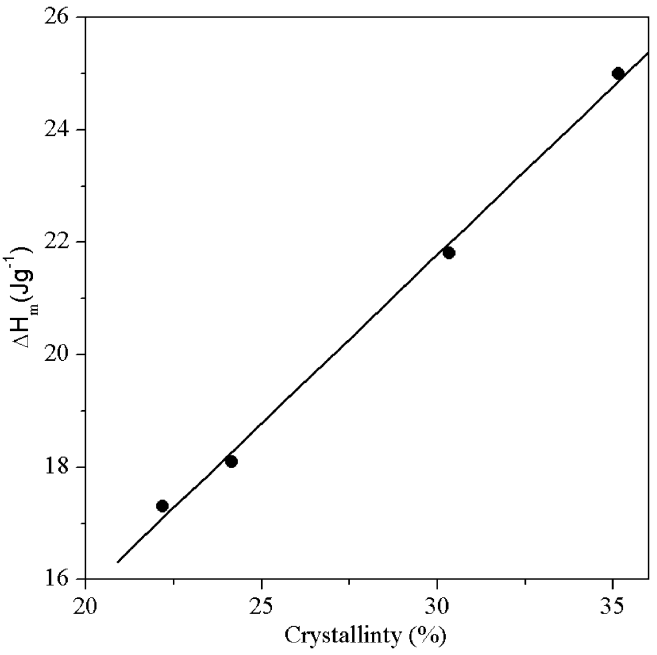

Fig. 8. Variation of heat of fusion with crystallinity of PC/PMMA blends.

where $\langle D \rangle$ is mean crystallite size, λ the radiation wavelength, θ the Bragg angle, $\beta(2\theta)$ the integral breadth of the diffraction profile expressed in angle 2θ and measured in radians. For Lorentzian peak shape, the integral breadth is related to the FWHM as given below [39,40]

$$\beta(2\theta) = 1.577 \cdot \mathrm{FWHM} \tag{2}$$

To obtain the integral breadth of the diffraction profile, we have subtracted the instrumental integral breadth from the observed integral breadth [36]. The variation of coherently scattering domain size so obtained with PMMA content is depicted in the inset (b) of Fig. 7. It is evident from this inset that the domain size increases with increasing PMMA content. This systematic variation in the coherently scattering domain size with PMMA content is observed for the Gaussian peak shape also even though the actual values of $\langle D \rangle$ differ by about ±2 Å. The increase in crystallite size is probably due to the forced crystallization of PMMA on PC crystallites which serve as templates. The interaction between the PMMA and PC chains is causing the ordered conformation of PMMA chains also, which increases the crystallite size.

4. Conclusion

Our XRD and DSC results show that as the PMMA content increases the crystallinity of the PC/PMMA blends and heat of fusion, decreases which is attributable to the glassy nature of PMMA. The 5% degradation temperature of the blends gradually shifts to lower temperatures for higher PMMA content. More significantly, the position of the XRD peak of PC at $2\theta \approx 17.22°$ shifts systematically towards the lower 2θ values with increasing PMMA content. The X-ray coherently scattering domain size, on the other hand, increases with increasing PMMA content of the blends. All these observations point towards the existence of specific interactions between the PC and PMMA phases in the blends.

Acknowledgements

We acknowledge the financial support from Department of Information Technology and Moser Baer India Limited (MBIL), India. Our special thanks are due to Mr. G.R. Nyati of MBIL and Dr. S.K. Mishra formerly of MBIL and now at SGI, Greater Noida. Helpful discussions with Dr. Nira Misra and Dr. B. Ray are also acknowledged.

References

[1] D.R. Paul, C.B. Bucknall, Polymer Blends, John & Sons, Inc., New York, 2000.
[2] L.A. Utracki, Polymer Alloys and Blends, Hanser, Munich, 1989.
[3] Y. Agari, A. Ueda, Y. Omura, S. Nagai, Polymer 38 (1997) 801.
[4] G.D. Butzbach, J.H. Wendorff, Polymer 32 (1991) 1155.
[5] J.S. Chiou, J.W. Barlow, D.R. Paul, J. Polym. Sci. B: Polym. Phys. 25 (1987) 1459.
[6] J.M. Saldanha, T. Kyu, Macromolecules 20 (1987) 2840.
[7] T. Kyu, J.M. Saldanha, Macromolecules 21 (1988) 1021.
[8] P. Sakellariou, G.C. Eastmond, Polymer 34 (1993) 1528.
[9] W.N. Kim, C.M. Burns, Macromolecules 20 (1987) 1876.
[10] E.M. Woo, C.C. Su, Polymer 37 (1996) 5186.
[11] M. Rabeony, D.T. Heeih, R.T. Garner, D.G. Peiffer, J. Chem. Phys. 97 (1992) 4505.
[12] N. An, Y. Yang, L. Dong, Macromolecules 40 (2007) 306.
[13] S.R. Ray, M. Bousmina, Macromol. Rapid Commun. 26 (2005) 1639.
[14] S.R. Ray, M. Bousmina, A. Maazouz, Polym. Eng. Sci. (2006) 1121.
[15] M. Penco, L. Sartore, S.D. Sciucca, L.D. Landro, A. D'Amore, Macromol. Symp. 247 (2007) 252.
[16] G. Montaudo, C. Puglisi, F. Damperi, J. Polym. Sci. A: Polym. Chem. 36 (1998) 1873.
[17] N. Marin, B.D. Favis, Polymer 43 (2002) 4723.
[18] D.S. Lim, T. Kyu, J. Chem. Phys. 92 (1990) 3944.
[19] M. Choi, K. Lee, J. Lee, H. Kim, Macromol. Symp. 249 (2007) 350.
[20] M. Okamoto, J. Appl. Polym. Sci. 80 (2001).
[21] M. Okamoto, J. Appl. Polym. Sci. 83 (2002) 2774.
[22] M.S. Lee, M.K. Ha, H.S. Lee, W.H. Jo, J. Korean Fiber Soc. 38 (2001) 101.
[23] T. Kyu, J.M. Saldanha, J. Polym. Sci.: Polym. Lett. 26 (1988) 33.
[24] T. Kyu, J.M. Saldanha, U.S. Patent 47,743,654.
[25] T. Kyu, U.S. Patent 5049,619.
[26] O. Olabisi, L.M. Robeson, M.T. Shaw, Polymer–Polymer Miscibility, Academic Press, New York, 1979.
[27] P. Viville, F. Biscarini, J.L. Breadas, R. Lazzaroni, J. Phys. Chem. B 105 (2001) 7499.
[28] M. Nishimoto, H. Keshkkula, D.R. Paul, Polymer 32 (1991) 272.
[29] E.M. Woo, C.C. Su, Polymer 37 (1996) 4111.
[30] W.P. Hsu, J. Appl. Polym. Sci. 80 (2001) 2842.
[31] T. Kyu, D.S. Lim, J. Chem. Phys. B 92 (1990) 3951.
[32] E.M. Woo, M.N. Wu, Polymer 37 (1996) 1907.
[33] G.R. Mitchell, A.H. Windle, Colloid Polym. Sci. 263 (1985) 280.
[34] A.H. Windle, Pure Appl. Chem. 57 (1985) 1627.
[35] H. Ouyanga, M.T. Wu, J. Appl. Phys. 96 (2004) 7066.
[36] L.E. Alexander, X-ray Diffraction Methods in Polymer Science, Wiley, New York, 1969.
[37] J. Font, J. Muntasell, Mater. Res. Bull. 35 (2000) 681.
[38] Y. Yoo, C. Park, J.C. Won, S.G. Lee, K.Y. Choi, J.H. Lee, Polym. Adv. Technol. 18 (2007) 1015.
[39] A.I. Gusev, A.A. Rempel, Nanocrystalline Materials, Cambridge International Science Publishing, 2004.
[40] R.L. Snyder, J. Fiala, H.J. Bunge, Defect and Microstructure Analysis by Diffraction, Oxford Science Publications, 1999.